EXPERIMENTAL INVESTIGATIONS ON MASONRY BUILDINGS STRENGTHENED USING FERRO-CEMENT OVERLAY UNDER DYNAMIC LOADING

Sachin B. Kadam (Corresponding Author)
Department of Applied Mechanics
Walchand College of Engineering
Sangli-416415, Maharashtra, India
E mail id: *sachin.kadam@walchandsangli.ac.in*

Yogendra Singh
Department of Earthquake Engineering
Indian Institute of Technology Roorkee
Roorkee-247667, Uttrakhand, India
E mail id: *yogendra.eq@gmail.com*

ABSTRACT

Use of Ferro-cement (Welded Wire Mesh in cement concrete/mortar) ‘splints’ and ‘bandages’ is a common method of retrofitting unreinforced masonry (URM) buildings in India. Indian code IS:13935 [22] provides pre-computed amount of reinforcement to be provided in the splints and bandages in URM buildings located in active seismic areas. However, adequacy of this technique is not comprehensively studied so far. In this research paper, behaviour of a half-scale burnt clay brick unreinforced masonry building and another similar building but retrofitted using carried out on ‘Shock Table’ test facility available at Department of Earthquake Engineering, Indian Institute of Technology Roorkee. In this facility, an impact is applied at the base of the specimen. Short duration impulse types of motion are the main characteristics of shock table. It also has low frequency content and higher base acceleration with respect to real ground motion. The crack pattern, weaker zones and modes of failure with increasing intensity of shaking, have been presented and conclusions are drawn with respect to effectiveness of the used strengthening technique. Equivalent frame models (EFM) of the tested scaled models have been developed in SAP2000 Nonlinear software and the numerical results are compared with the prototype results. The results suggest that the lateral load resistance of the retrofitted building increases considerably, as compared to the URM buildings. The EFMs are able to predict the peak displacement, quite reasonably but fail to predict the response waveform.

KEYWORDS: Unreinforced Brick Masonry; Shock Table Test; Wire-Mesh, Retrofit; Equivalent Frame Model

INTRODUCTION

The adequacy of a retrofitting method can be fully tested either during a real earthquake, or by full scale model testing on a shake-table, simulating the expected ground motion. Non-availability of full/large scale shake-table testing facilities, at many places, necessitates the use of scaled models and simplified testing procedures. These scaled models have been successfully used to compare the dynamic behaviour of URM and strengthened models [Paulson et al. (1) ; Nikolic-Brzev and Arya (2); Tomaževič et al. (3); Ersubasi and Korkmaz (4); Mendes et al. (5)]. In India these scale models have been successfully tested on shock-table facility [Arya (6); Qamaruddin et al. (7); Qamaruddin et al. (8); Agarwal and Thakkar (9); Jagdish et al. (10)]. In the present study, two models of half scale brick masonry, one without any strengthening and the other with strengthening using Ferrocement in splints and bandages, have been tested and apprise with the analytical simulation using macro-modeling approach named “Equivalent Frame Method”. The models have been tested for a series of shocks of gradually increasing intensity on Shock-Table facility available at the Department of Earthquake Engineering, IIT Roorkee. Agarwal [11], Masood [12], and Dubey [13] have shown that the shock-table motions are has low frequency content and higher base acceleration. These motions typically have much lower damage potential than a real earthquake motion having identical peak ground acceleration. However, this testing is useful in identifying the pattern of cracking, weak zones in the structure, modes of failure subjected to base excitation, and damage with increasing intensity of shaking; and useful conclusions can be drawn with respect to efficacy of the strengthening technique. In this paper strengthening technique using Welded Wire Mesh in cement concrete/mortar for 'splints' and 'bandages have been tested for dynamic loading. This technique is already has been verified at component level [Kadam et. al (14), Kadam et. al (15)] and also meticulously extended over existing masonry school building [Kadam et. al (16)]. A direct comparison of the performance of the URM and retrofitted models can be made by testing both of the models simultaneously subjected to the same shock. To accommodate both these models on same shock-table platform and to keep the total weight within maximum pay load of the shock-table, half scale models made of specially manufactured bricks have been used.

CONSTRUCTION OF MODELS FOR SHOCK-TABLE TEST

To study the effectiveness of strengthening technique using Welded Wire Mesh in cement concrete/mortar for 'splints' and 'bandages', two models were constructed simultaneously on the shock-table. A skilled mason was employed to construct the specimens with half scale burnt clay bricks of size 118×58×37 mm and 8-10 mm thick mortar joints using 1:6 cement-sand mortar. Curing was done for 28 days and the models were tested in dry condition. Table 1 shows the details of the models. Model 1 represents a single room building built in traditional way as a ordinary house. Model 2 was constructed with seismic strengthening using Ferrocement strips in splints and bandages.

Table 1: Detail of Conventional and Strengthened Replica

Sr. No.	Scale of Model	Description of the Replica
Model 1	Half Scale	Conventional brick masonry replica in 1:6 cement-sand mortar without any earthquake resistant feature
Model 2	Half Scale	Brick masonry replica in cement-sand mortar proportionate as 1:6, with strengthening using Ferrocement strips in splints and bandages

EXPERIMENTAL SET-UP

The general arrangement of the shock-table test facility, available at IIT Roorkee, has been shown in Figure 1. The test facility consists of i) Permanent way, ii) Shock-table platform, iii) Dead load wagons, and iv) Winch mechanism to pull the wagons as major components.

The permanent way consists of a railway track having three lengths of 12 m each of 44.6 kg/m rails. Thus total weight of one track is 1605.6 kg. The rails are laid on prestressed concrete sleepers. The rails are placed at a spacing of 1.676 m at the inner face, and with a grade of about 8 %. The rails have been marked at an interval of half meter to control the intensity of impact by positioning and releasing of the wagons at desired location. The prestressed concrete sleepers rest on a well-prepared base, which is about 150 mm thick, made up of stone ballast directly laid on the soil.

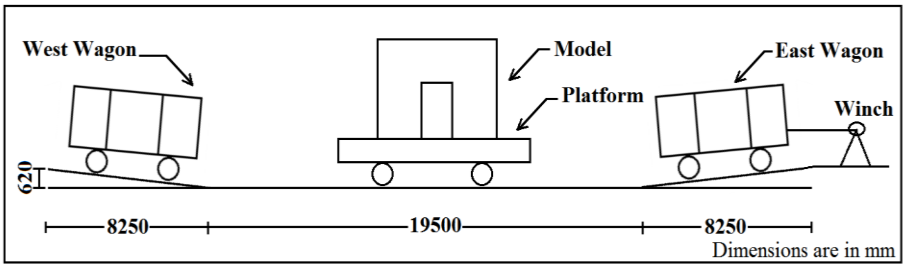

Fig. 1 Line sketch of shock-table test facility, available at the Department of Earthquake Engineering, Indian Institute of Technology (IIT) Roorkee

The shock-table platform consists of an open railway wagon chassis weighing 8.5 tonnes with a rigid steel platform, 7×6 m in plan. Ten helical coil compression springs have been mounted on each end of the Shock-Table platform to moderate the impact from the loading wagon. Each spring's stiffness is of the order of 138 kg/mm with a capacity of 7.5 tonnes. The maximum acceleration of the table has been recorded around 10 g (98.1 m/s^2) in some previous conducted tests on the platform. Two loading wagons have been placed on the track on both the sides of the shock-table platform. The East side wagon used to apply the impact which moves along track using winch arrangement as shown in Figure 1. This wagon has been loaded with boulders, sand and reinforced brick slab with the total weight approximating to about 35 tonnes. The West side wagon is stationary and has been loaded with boulders and sand, weighing about 30 tonnes. During the test, the East side loaded wagon has been pulled up the slope and allowed to roll down to give an impact to the shock-table through springs. In the process, the structure constructed on the shock-table platform gets a few shocks, one main shock by the initial impact and then subsequent shocks by rebounds with the stationary and the loading wagons. A manually operated portable winch has been used to pull the dead load wagons up on the inclined slope. On the grades of about 8 % with friction, a pull of about 3500 kg is required. A mechanism to release the loading wagon for rolling down, using a sharp blow from a hammer, has been provided. A safety pin in the release mechanism and stoppers made of steel under wagon wheels have been used to safeguard against accidental release.

TESTING PROCEDURE AND INSTRUMENTATION

As test code of conduct gradually increasing intensity shocks are imparted to the platform on which the model is built, by the heavily loaded East end wagon. One single impact from end wagons imparts a triangular shaped pulse to the central wagon (platform). The first pulse is imparted by the East end wagon and depending on the energy of the impact, subsequent pulses are imparted from rebound with the platform and West end wagons. The intensity of the shock has been controlled, by calibration marks on the rail and the springs mounted on the shock-table. The acceleration time histories of the models were recorded during each shock. The cracks developed at various shocks were marked to study the pattern of cracking and the mode of failure. The models were constructed side by side on the ‘Shock-Table’ and both the models were subjected to shock type motion at the base simultaneously as shown in Figure 2.

Fig. 2 Photograph showing the completed models on shock-table platform

The models were instrumented for measurement of accelerations at top and bottom, during the dynamic testing. For the measurement of accelerations with time, four accelerometers were deployed. These accelerometers were connected to an eight channel data acquisition system for synchronized measurement. Out of these four accelerometers, two were used to measure accelerations of platform (placed on the base of models) and remaining two were used for measurement of accelerations of top of the models (placed on the roofs of the models). The relative displacement between the platform and the model top during successive shocks was obtained from this acceleration data (using double integration).

EXPERIMENTAL OBSERVATIONS

The building models were subjected to shocks of increasing intensity. The intensity of shocks was controlled by moving the loading (East end) wagon to different distances up the inclined before releasing. For the first shock, the velocity of central wagon (Shock-Table Platform) was not adequate to cause a collision with the stationary (West end) wagon. As a result, only one pulse was applied in the first shock. In successive shocks, the velocity of the platform was adequate to cause a collision with the stationary wagon and two or more pulses were applied. Collapse of the conventional (unreinforced) model occurred after the third shock. The strengthened model was subjected to two more shocks, with maximum acceleration up to 10 g (98.1 m/s^2). The model could not be tested up to collapse as higher accelerations could not be achieved using the available test facility. The traditionally constructed model proved very fragile, but the performance of retrofitted model is substantially improved. Major cracks were seen in the traditional model at the second shock where peak base acceleration of 9.99 m/s^2 was applied during the first pulse and acceleration of 8.38 m/s^2 was applied during the rebound pulse. The major roof acceleration of the traditional model was 18.98 m/s^2 in loading cycle and 13.05 m/s^2 during rebound cycle. During this shock, formation of cracks was observed in the traditional model as shown in Figure 3. The cracks starting from the top corner of the door opening extended up to the corner of wall. Similar cracks were also seen in the opposite shear wall having window opening. The solid walls orthogonal to the pulse excitation were subjected to out-of-plane inertia forces. No damage was observed in the retrofitted masonry model, up to this shock, as shown in Figure 3.

Fig. 3 Formation of cracks in traditional model whereas retrofitted model was intact after shock 2

In the third shock, the peak acceleration of 24.67 m/s^2 was applied at the base of the models during loading cycle, and an acceleration of 18.96 m/s^2 was applied during the rebound cycle. The major roof acceleration of the retrofitted model was 32.85 m/s^2 in loading cycle and 21.43 m/s^2 during rebound cycle.

Fig. 4 Front view of the shock-table platform showing the traditional and retrofitted models after shock 3. The traditional model collapsed under this shock

The traditional masonry model collapsed during this shock, and no damage was observed in the retrofitted model as depicted in Figure 4. It was also noted by observing the closer view of the retrofitted model, that no cracks visible by naked eye. In the fourth and fifth shock, the intensity of the impact loading was kept on increasing up to possible capacity of shock table. Maximum possible peak base acceleration in the fifth shock was observed to be 100.67 m/s^2 in loading cycle. There was no damage to strengthened model during shock 4 but minor damage was observed to the strengthened model during fifth shock. Horizontal cracks originating from the base of the door opening present on shear wall on south side (Figure 5). Initiation of diagonal cracks was also observed as shown in Figure 5. The initiation of diagonal cracks from the corners of the window opening was also observed on northern side of the retrofitted model. However, there was no visible wreckage to the east and west side solid strengthened walls.

Fig. 5 Front view of shock-table platform showing view of minor cracks developed in retrofitted models after shock 5 on southern side

Inputs shocks were measured with four accelerometers deployed at different location and results of five input shocks at base of the models have been depicted in Figure 6.

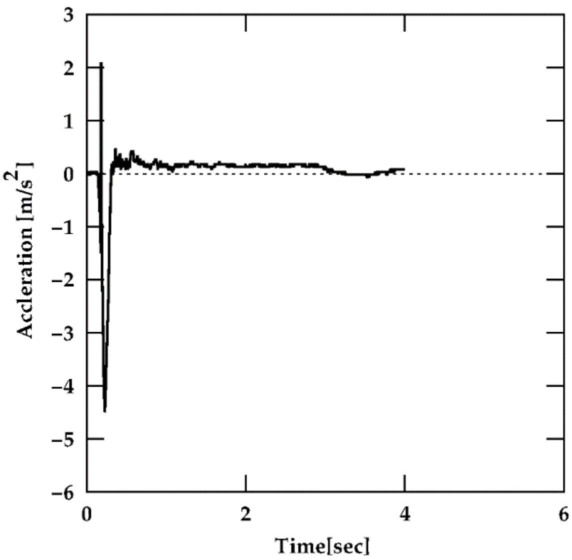

(a)

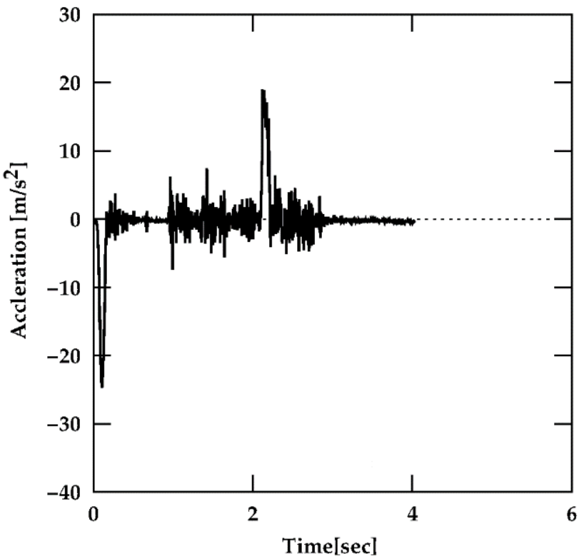

(b)

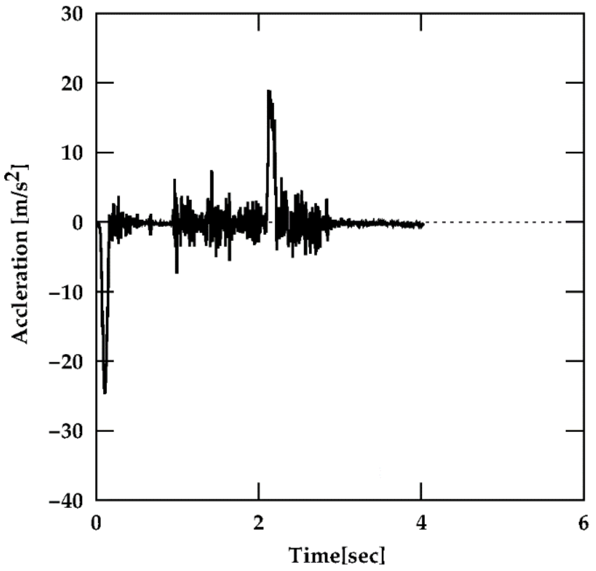

(c)

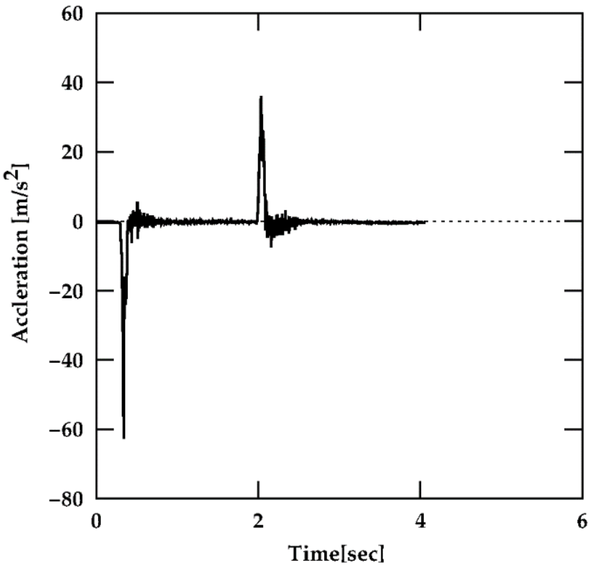

(d)

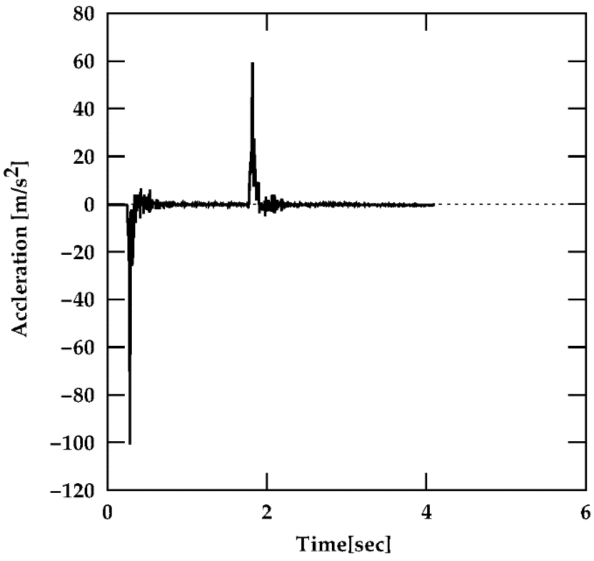

(e)

Fig. 6 Input accelerations measured at the base of (a) URM model subjected to Shock 1, (b) URM model subjected to Shock 2, (c) Retrofitted model subjected to Shock 3, (d) Retrofitted model subjected to Shock 4, and (e) Retrofitted model subjected to Shock 5

ANALYTICAL SIMULATION OF SHOCK-TABLE TEST

Macro-modelling technique “Equivalent Frame Model” (EFM), which provides an easier visualization of the structural behaviour and reasonably accurate results with moderate computational efforts has been used in simulation of shock table test. To develop the EFM of a URM wall, Dolce [17] presented the concept of effective height of piers. The Dolce’s criterion for computation of effective height of piers is shown in Figure 7 and can be expressed as

$$H_{eff} = h' + \frac{1}{3h} D(H - h') \tag{1}$$

where, the variables for given pier are referred from Figure 7. The flexural capacity, M_u diagonal shear capacity, $V^f{}_u$ and the sliding shear capacity $V^s{}_u$, of a URM pier can be obtained [Pasticier et al. (18)] as

$$M_u = \frac{\sigma_o D^2 t}{2}\left(1 - \frac{\sigma_o}{k f_d}\right) \tag{2}$$

$$V^f{}_u = \frac{1.5 f_{vod} Dt}{\xi}\sqrt{\left(1 + \frac{\sigma_o}{1.5 f_{vod}}\right)} \tag{3}$$

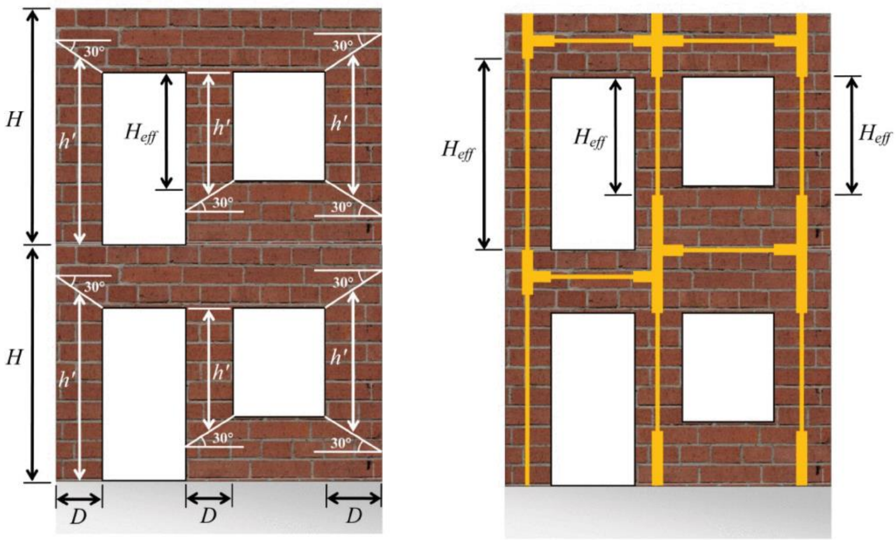

(a) (b)

Fig. 7 Schematic 2d diagram of a typical masonry wall showing (a) Definition of effective height of piers dolce [17], and (b) equivalent frame model

$$V^s{}_u = \frac{1.5 f_{vod} + \dfrac{\mu \sigma_o}{\gamma_m}}{1 + \dfrac{3H_o}{D\sigma_o} f_{vod}} \tag{4}$$

where, σ_o is the axial stress on the pier, *D* is the length of the pier, *t* is the thickness of the pier, *k* is the coefficient considering axial stress on toe of the pier (generally assumed as 0.85), f_d is the compressive strength of the pier, f_{vod} is the design shear strength with zero axial stress, ξ is the ratio *D/t* of length to thickness of the pier, μ is the friction coefficient (assumed as 0.4), H_o is the effective height of the pier and γ_m is the factor of safety (assumed equal to 2.0).

The equivalent 3D frame model of the scaled building on shock table platform is shown in Figure 8. The nonlinear behaviour of piers and spandrels has been modelled by assigning plastic hinges [Prasad (19); Prasad et al. (20); Singh et al. (21)] at preconceived locations in the equivalent frame elements. The major limiting concerned of EFM was its incompetence in simulation the effect of changing axial stresses while estimating rocking and shear capabilities of piers. This limitation has been overcome in the present study by using a set of two P-M (axial force versus bending moment) interaction hinges to simulate the combined behaviour in rocking, sliding and diagonal shear as illustrated in earlier studies. [Prasad (19), Singh et al. (21), Kadam et al. (16)].

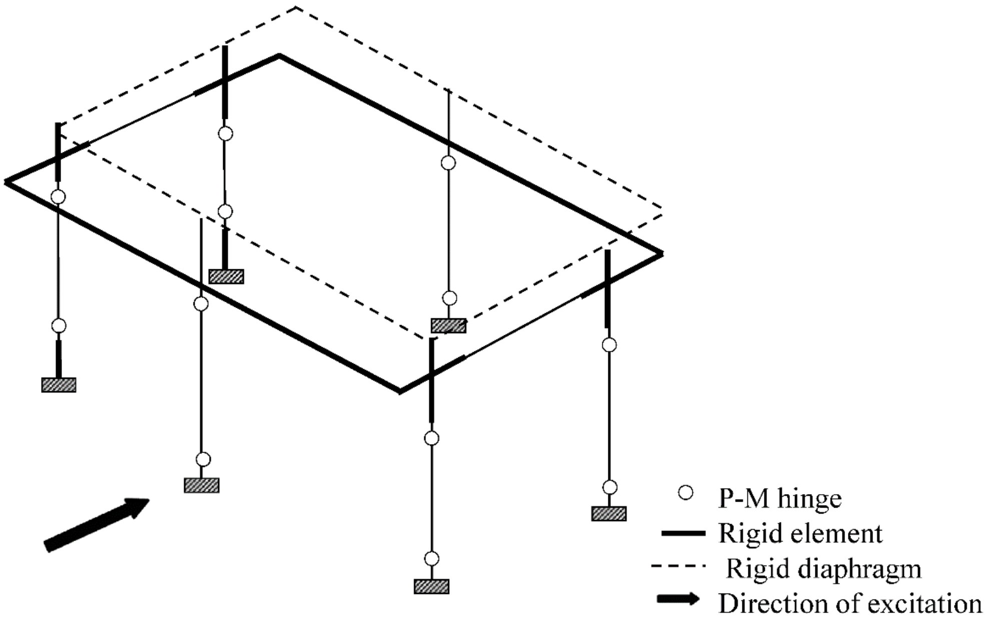

Fig. 8 3D Equivalent frame model of the buildings tested on shock-table platform

The P-M interaction hinges are assigned a yield curve representing the governing failure mode (i.e. the one having minimum capacity) at a given axial force in the pier. It is to be noted that for a given pier, different modes of failure may govern the behaviour at different values of axial force. The capacities of piers in rocking, diagonal shear and sliding shear, for varying axial force have been computed using Equations 2-4.

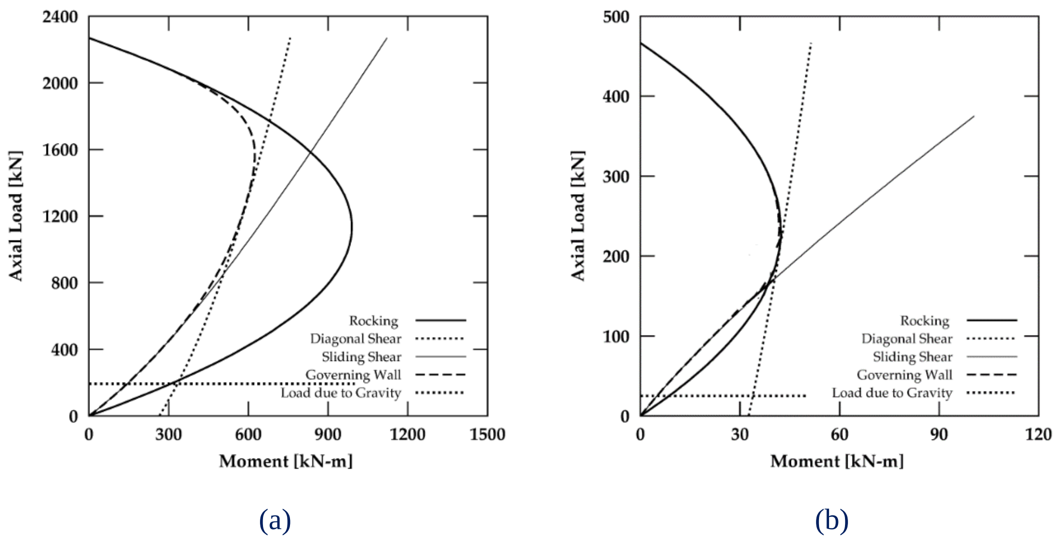

Fig. 9 Axial load-moment (p-m) interaction curves for (a) squat pier, and (b) slender pier

Yielding will occur in the mode having minimum capacity for given value of axial force. Different combinations of P-M hinges in a pier have been considered as the minimum of moment capacity developed from flexural or shear actions at the particular level of axial load. For the demonstration P-M interaction curves has been depicted in Figure 9 for typical squat and slender piers. Having considered all possible failure envelop (rocking, sliding and diagonal shear) lower bond envelop has been shown in these two cases by thick dotted line. The horizontal dotted line is also shown in this Figure 9 to quantify axial force due to gravity on these piers. Note that this axial force is expected to vary during the action of lateral load, due to overturning action of the building. The variation will be small in the case of a low rise building but can be significant in the case of a slender building. The detailed case study on squat and slender piers in existing building are available in Kadam et. al [16].

For seismic performance enhancement of the existing building, the URM walls have been strengthened in in-plane and out-of-plane action using the Ferrocement strips. The retrofit design has been performed using the concept of permissible stresses as per IS 1905 [23] and IS 456 [24]. The quantification of reinforcement in splints and bandages has been realized by considering the composite action of the masonry and WWM [Singh (25)]. The detailed calculations of the reinforcement in different splints and bandages in a typical wall of the masonry building, are available in Kadam [26] and not presented here for brevity. In mathematical modelling of simulation of retrofitted masonry the earlier equations proposed by Ghaissi [Ghiassi (27)] has been used as many similar aspects were observed in both these works.

The ordinary beam theory has been utilized to establish moment-curvature (M-ϕ) curve for the composite masonry-micro-concrete-WWM section. This theory is used by assuming linear distribution of strain across the section and compatibility of strain across the cross-section.

The diagonal shear strength of the strengthened masonry pier has been obtained [ASCE 41-06 (28); FEMA 356 (29); MSJC (30)] as

$$V_{nm} = 0.083\times\left[4.0-1.75\left(\frac{M_u}{V_u d_v}\right)\right]A_{nv}\sqrt{f'_m}+(0.53\sqrt{f'_c}\,t_c d)+(0.5 f_y A_v \frac{d_v}{s})+(0.25P_u) \tag{5}$$

where, V_u and M_u are the applied shear force and bending moment, respectively, on the wall section, d_v is the effective length of the wall, usually considered equal to 0.8 times of the total length of the wall. For cantilever walls, the term $\frac{M_u}{V_u d_v}$ is equal to the aspect ratio of the wall. A_{nv} is the net mortared area, f'_c is the compressive strength of mortar, A_v is the area of vertical reinforcement, *s* is the spacing of the reinforcement, and f'_m is the compressive strength of strengthened masonry which is governed by effective modulus of elasticity of strengthened masonry (E_{rm}). In absence of more accurate estimates, it can be taken as [Ghiassi (27)]

$$f'_{rm} = \varepsilon_u E_{rm\sec} \tag{6}$$

where, ε_u is the peak strain in masonry and can be considered equal to 0.003, $E_{rm\sec}$ is the secant modulus of elasticity that can be assumed equal to half of the initial modulus of elasticity of the strengthened masonry. The initial modulus of elasticity of the strengthened masonry can be computed [Ghiassi (27)] as follows,

$$E_{rm} = \left(-0.068\frac{t_m}{t_c}+1.068\right)\left(0.243\frac{E_m}{E_c}+0.45\frac{E_b}{E_c}+0.335\right)E_c \tag{7}$$

where, t_m is the thickness of the masonry wall, t_c is the concrete layer thickness, E_m is the modulus of elasticity of the mortar, E_b is the modulus of elasticity of bricks, and E_c is the modulus of elasticity of concrete. The strengthened masonry walls with low axial loads and longitudinal reinforcement ratio are prone to sliding shear failure. The capacity of strengthened wall due to sliding shear failure is given by Ghiassi et al. [31] as

$$V_{se} = \mu_1 P_u + \mu_2 A_{vf} f_{ye} \tag{8}$$

where, P_u is the axial load on the wall, A_{vf} is the area of reinforcing bars perpendicular to the sliding plane, f_{ye} is the expected yield strength of reinforcing bars, μ_1 is the coefficient of friction of brick masonry, and μ_2 is the coefficient of friction of concrete, that can be taken equal to 0.9.

Benedetti et. al [32] carried out large experimental programme in which they have conducted shaking-table tests on 119 scaled masonry buildings. After suffering damage, the models were repaired and strengthened and tested again. The study gives tentative idea about damping of the fundamental modes which varies from 6 % to 10 % to critical for undamaged brick masonry, Further these values were confirmed between 10-12 % for damaged brick masonry.

Elmenshawi et. al [33] carried out test on stone masonry core and they came with opinion that the viscous damping ratio is damage dependent, and can be modeled by mass proportional damping in dynamic analysis to account for existing damage in a structure.

As mentioned earlier, the models have been constructed using half scale bricks, specially manufactured for this purpose. Tests on half scale brick masonry with the same bricks and mortar proportion were performed by Masood [12]. Basic material properties such as compressive strength (σ_c), modulus of elasticity *(E)* and Poisson's ratio (ν) used in modeling have been considered from this work. Nonlinear Dynamic analysis has been performed to estimate the response of the models, subjected to recorded excitations. As mentioned earlier, the shock-table motion is characterized by high frequency content. Accordingly, a shorter time step (0.0001 sec) has been used in the step-by-step time integration. Damping was considered by the classical Rayleigh formulation, and a 10 % damping ratio on the first two modal shapes was selected as suggested by Benedetti et. al [32]. Further this Rayleigh damping of 10 % has been used in both the models which have been subjected to identical shocks recorded at the shock-table platform. The output from the time history analysis was obtained in the form of displacement-time record at roof level. This output displacement has been compared with experimentally obtained displacement.

COMPARISON OF NUMERICAL AND EXPERIMENTAL RESULTS

Figures 10 and 11 show the plastic hinge patterns in the analytical models of the traditional (unreinforced) and retrofitted buildings subjected to different shocks. In the 1995, Structural Engineers Association of California published a document called Vision 2000-Performance based seismic engineering of buildings. It is applicable to the rehabilitation of existing buildings as well as to the design of new buildings. The different limit states, considered as performance level are (Immediate Occupancy) 'IO', (Life Safety) 'LS' and (Collapse Prevention) 'CP' represent the damage states in terms of the thresholds (acceptance criteria) defined in FEMA 356 [29] for traditional model and as per Ghiassi et. al [31] and Kadam et. al [16] for the retrofitted model. It can be seen from the figures that the observed hinge pattern matches very well with the damage observed during testing. For the unreinforced (traditional) building model subjected to Shock 2, the plastic hinges in all the piers reach 'CP' level, indicating imminent collapse as shown in Figure 10 (b). The solution for Shock-3 could not converge for the traditional building, indicating collapse.

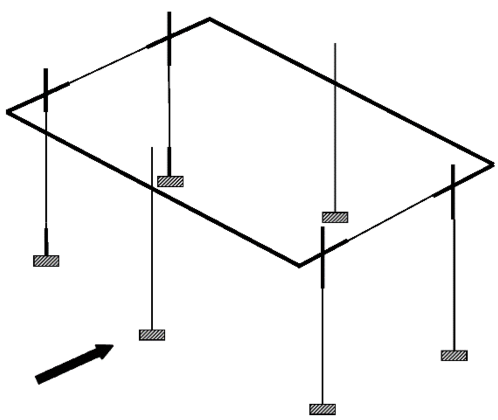

(a)

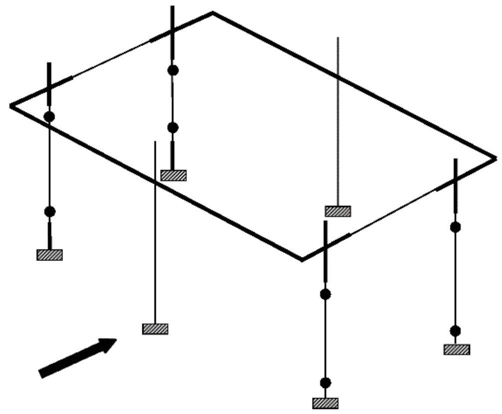

(b)

IO LS CP

Fig. 10 Plastic hinge patterns in traditional building model subjected to: (a) shock-1, and (b) shock-2

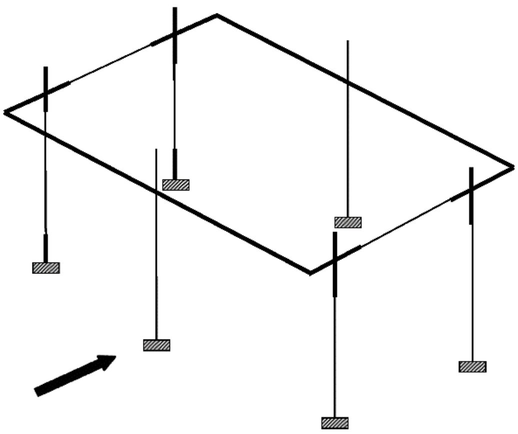

(a)

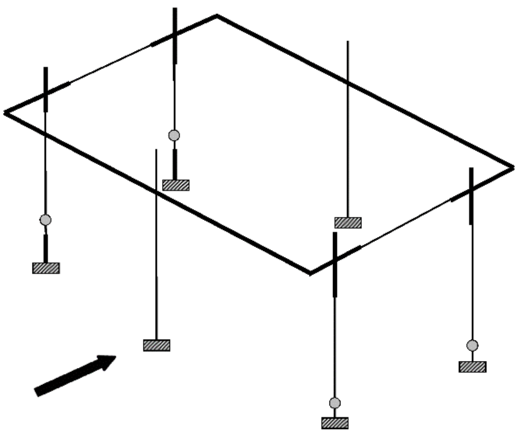

(b)

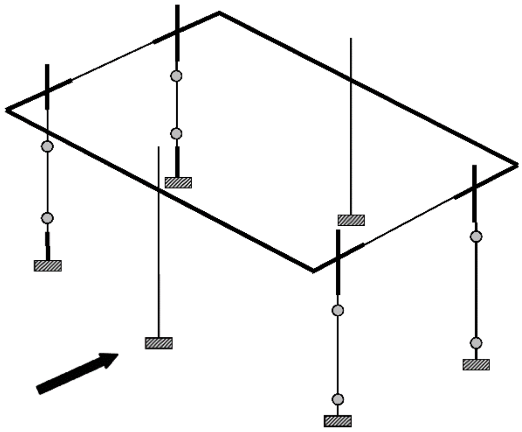

(c)

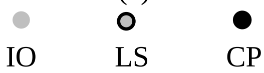

Fig. 11 Plastic hinge patterns in retrofitted building model subjected to: (a) shock-3, (b) shock-4, and (c) shock-5

On the other hand, for the retrofitted building, no yielding of plastic hinges occurs until Shock-4 as shown in Figure 11(a) and 11(b). For the higher intensity shocks, the plastic hinges in piers show yielding, but did not cross the 'Life Safety' performance level even for Shock-5 as shown in Figure 11(c). This is in good match with the no damage observation for Shock-3 and minor damage observed under Shock-5 for this building during the actual test.

Comparison of numerical and experimental displacement-time plots for shocks of increasing intensity is shown in Figures 12-16. Displacements for Shock-1 and Shock-2 are compared for the traditional (URM) model, whereas for larger shocks, the response of the retrofitted model has been compared, as the traditional model collapsed during Shock-3.

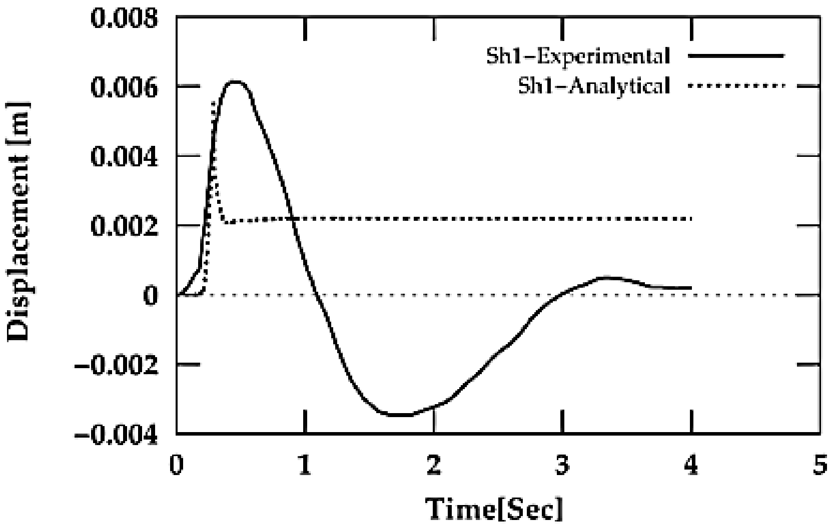

Fig. 12 Comparison of displacement response of traditional model for shock-1

Figure 12 compares the analytical and observed displacement response of traditional model subjected to Shock 1. A permanent displacement of about 2 mm is observed, and the vibrations stopped much earlier than that in the experiment. However, as shown earlier in Figure 10(a), no yielding in any component has been observed in the analysis. As the first shock was of very low intensity, the actual damping mobilized is much lower than the 10 % assumed in the analysis. The numerically obtained displacement waveform, in this case indicates higher than the actual damping in the numerical model and presence of some noise in the input.

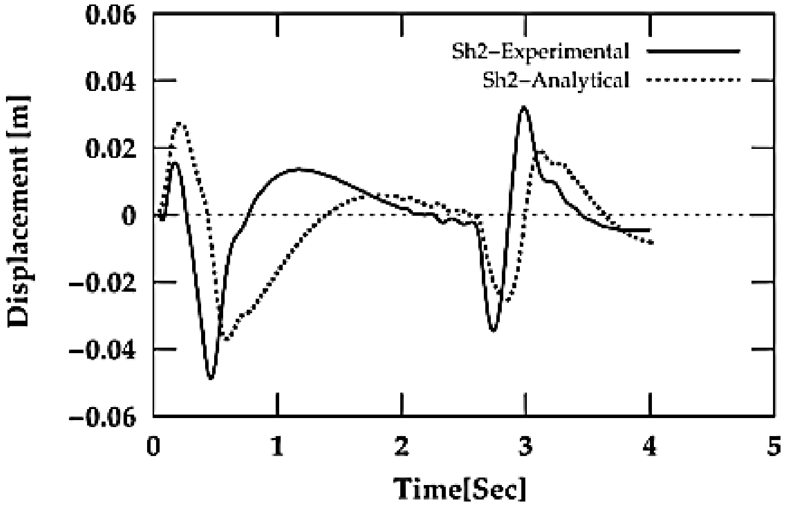

Fig. 13 Comparison of displacement response of traditional model for shock-2

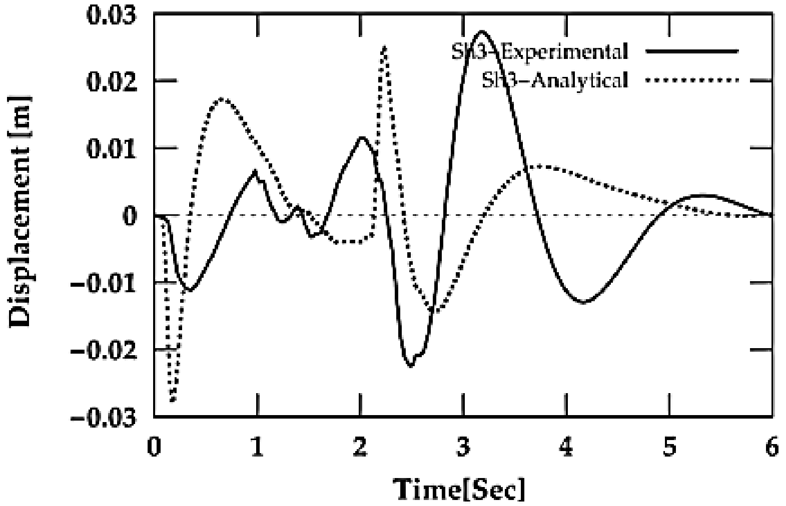

Fig. 14 Comparison of displacement response of retrofitted model for shock-3

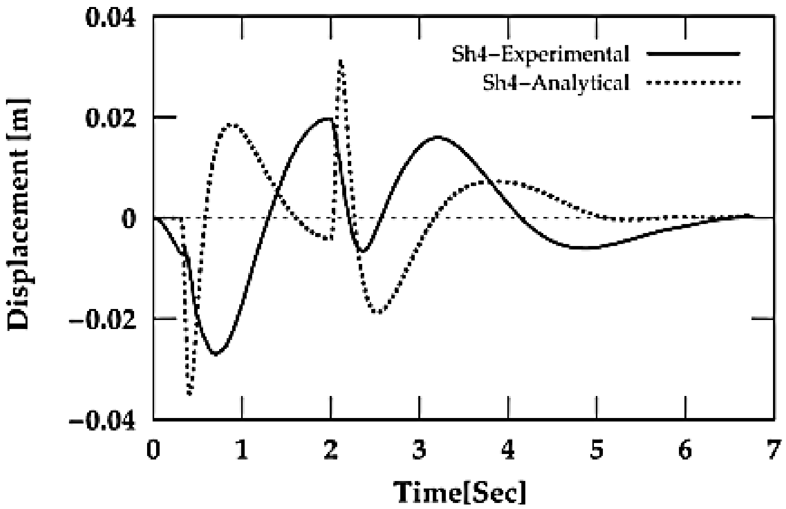

Fig. 15 Comparison of displacement response of retrofitted model for shock-4

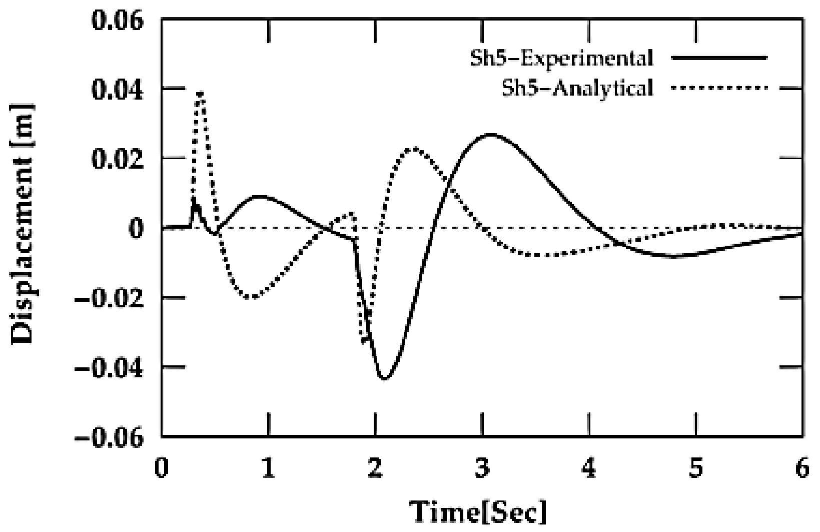

Fig. 16 Comparison of displacement response of retrofitted model for shock-5

On the other hand, the numerical and experimental displacements for Shock-2 match quite closely, indicating a close prediction of the stiffness and damping for this level of shaking which corresponds to significant yielding and cracking in the masonry model (Figure 3). The difference in the numerical and experimental displacement waveform increases for the higher intensity shocks. However, the peak displacements observed numerically and experimentally are in good agreement for all the shocks.

SUMMARY

Major cracks were seen in the traditional model at Shock-2 (peak acceleration = 1 g) and collapse occurred at Shock-3 (peak acceleration = 2.5 g), whereas, the retrofitted model survived up to Shock-5 (peak acceleration = 10 g) with minor cracks. It is to be noted that the models can survive much higher peak accelerations in the shock-table test, as compared to the earthquake ground motions, due to low damage potential of the high frequency impulse motions in case of shock-table test. The numerical analysis using Equivalent Frame Approach, predicted the damage levels in both the building models with reasonable accuracy at all the shaking levels, justifying its application for estimating seismic performance of URM and retrofitted buildings. The Equivalent frame models also predicted the peak displacements quite close to those obtained experimentally, for both URM and strengthened buildings. However, the displacement-time waveform could not be predicted accurately.

ACKNOWLEDGEMENTS

The financial support received from Temasek Foundation, Singapore for conducting the study is gratefully acknowledged.

REFERENCES

1. Paulson, T., Abrams, D. and Mayes, R. (1991). “Shaking-Table Study of Base Isolation for Masonry Buildings”, *Journal of Structural Engineering, Vol. 117, No. 11, pp. 3315-3336*.
2. Nikolic Brzev, S. and Arya, A.S. (1996). “Seismic Isolation of Masonry Buildings - An Experimental Study”, *Proc., Eleventh World Conference on Earthquake Engineering*.
3. Tomaževič, M., Klemenc, I. and Weiss, P. (2009). “Seismic Upgrading of Old Masonry Buildings by Seismic Isolation and CFRP Laminates: a Shaking-Table Study of Reduced Scale Models”, *Bulletin of Earthquake Engineering, Vol. 7, No. 1, pp. 293-321*.
4. Ersubasi, F. and Korkmaz, H.H. (2010). “Shaking Table Tests on Strengthening of Masonry Structures Against Earthquake Hazard”, *Natural Hazards and Earth System Sciences, Vol. 10, No. 6, pp. 1209-1220*.

5. Mendes, N., Lourenço, P.B. and Campos-Costa, A. (2014). "Shaking Table Testing of an Existing Masonry Building: Assessment and Improvement of the Seismic Performance", *Earthquake Engineering & Structural Dynamics, Vol. 43, No. 2, pp. 247-266*.
6. Arya, A.S. (1984). "Sliding Concept for Mitigation of Earthquake Disaster to Masonry Buildings", *Paper Read at 8 WCEE, at San Francisco, California*.
7. Qamaruddin, M., Arya, A.S. and Chandra, B. (1984). "Dynamic Testing of Brick Buildings Models", *Proc., The Institution of Civil Engineers, pp. 353-365*.
8. Qamaruddin, M., Arya, A.S. and Chandra, B. (1986). "Seismic Response of Brick Buildings with Sliding Substructure", *Journal of Structural Engineering, Vol. 112, No. 3, pp. 558-572*.
9. Agarwal, P. and Thakkar, S.K. (2001). "A Comparative Study of Brick Masonry House Model Under Quasi-Static and Dynamic Loading", *ISET Journal of Earthquake Technology, Vol. 38, No. 2-4, pp. 103-122*.
10. Jagdish, K.S., Raghunath, S. and Nanjunda Rao, K.S. (2002). "Shock Table Studies on Masonry Building Model with Containment Reinforcement", *Journal of Structural Engineering, Vol. 29, No. 1, pp. 9-17*.
11. Agarwal, P. (1999). "Experimental study of Seismic Strengthening and Retrofitting Measures in Masonry Buildings", *Ph.D., University of Roorkee, Roorkee*.
12. Masood, A. (2006). "Out of Plane Behaviour of Unreinforced Masonry Infill Panels", *Ph.D. Thesis, Indian Institute of Technology Roorkee, Roorkee*.
13. Dubey, R.N. (2011). "Experimental Studies to Verify the Efficacy of Earthquake Resistant Measures in Masonry Buildings", *Ph.D. Thesis, IIT Roorkee, Roorkee*.
14. Kadam, S.B., Singh, Y. and Li, B. (2014). "Strengthening of Unreinforced Masonry Using Welded Wire Mesh and Micro-Concrete – Behaviour under In-Plane Action", *Construction and Building Materials, Vol. 54, pp. 247-257*.
15. Kadam, S., Singh, Y. and Li, B. (2015). "Out-of-Plane Behavior of Unreinforced Masonry Strengthened Using Ferrocement Overlay", *Materials and Structures, Vol. 48, No. 10, pp. 3187-3203*.
16. Kadam, S.B., Singh, Y. and Bing, L. (2020). "Seismic Fragility Reduction of an Unreinforced Masonry School Building Through Retrofit Using Ferrocement Overlay", *Earthquake Engineering Engineering Vibration 19, pp. 397–412, https://doi.org/10.1007/s11803-020-0569-7.*
17. Dolce, M. (1989). "Schematizzazione E Modellazione Per Azioni Nel Piano Delle Pareti (Models for In-Plane Loading of Masonry Walls)", *Corso Sul Consolidamento Degli Edifici in Muratura In Zona Sismica, Ordine Degli Ingegneri, Potenza, (Quoted in Magenes and Della Fontana, 1998).*
18. Pasticier, L., Amadio, C. and Fragiacomo, M. (2008). "Non-Linear Seismic Analysis and Vulnerability Evaluation of a Masonry Building by Means of the SAP2000 V.10 code", *Earthquake Engineering & Structural Dynamics, Vol. 37, No. 3, pp. 467-485*.
19. Prasad, J.S.R. (2009). "Seismic Vulnerability and Risk Assessment of Indian Urban Housing", *Ph.D. Thesis, Indian Institute of Technology Roorkee, India*.
20. Prasad, J.S.R., Singh, Y., Kaynia, A.M. and Lindholm, C. (2009). "Socioeconomic Clustering in Seismic Risk Assessment of Urban Housing Stock", *Earthquake Spectra, Vol. 25, No. 3, pp. 619-641*.
21. Singh, Y., Lang, D.H., Prasad, J. and Deoliya, R. (2012). "An Analytical Study on the Seismic Vulnerability of Masonry Buildings in India", *Journal of Earthquake Engineering, Vol. 17, No. 3, pp. 399-422*.
22. IS 13935 (2009). "Indian Standard code of Evalution,Repair and Strengthening of Masonry Building", *Bureau of Indian Standards, IS13935, New Delhi, India*.
23. IS 1905 (1987). "Indian Standard Code of Practice for Structural Use of Unreinforced Masonry (Third Revision)", *Bureau of Indian Standards, IS1905,* New Delhi, India.
24. IS 456 (2000). "Plain and Reinforced Concrete - Code of Practice", *Bureau of Indian Standard, IS 456, New Delhi. India*.
25. Singh, Y. (2011). "Seismic Retrofit of Unreinforced Masonry Buildings - Guidelines for Engineers", *Centre of Excellence in Disaster Mitigation and Management, IIT Roorkee, India*.

26. Kadam, S.B. (2015). "Seismic Evaluation and Retrofit of Masonry Buildings", *Ph.D. Thesis, Indian Institute of Technology Roorkee, India*.
27. Ghiassi, B. (2009). "Homogenization and Development of Constitutive Models for Seismic Evaluation of Brick Masonry Structures Retrofitted with Reinforced Concrete Layer", *M.Sc. Thesis., Tarbiat Modares Univ., Tehran, Iran*.
28. ASCE 41-06 (2007). "Seismic Rehabilitation of Existing Buildings", *American Society of Civil Engineers, Virginia, USA*.
29. FEMA 356 (2000). "Prestandard and Commentary for the Seismic Rehabilitation of Buildings", *Federal Emergency Management Agency, Washington, D.C., USA*.
30. MSJC, (2013). "Building Code Requirements and Specification for Masonry Structures", *TMS 402-13/ACI 530-13/ASCE 5-13, The Masonry Society*.
31. Ghiassi, B., Soltani, M. and Tasnimi, A. (2012). "Seismic Evaluation of Masonry Structures Strengthened with Reinforced Concrete Layers", *Journal of Structural Engineering, Vol. 138, No. 6, pp. 729-743*.
32. Benedetti, D., Carydis, P. and Pezzoli P. (1998). "Shaking Table Tests on 24 Simple Masonry Building", *Earthquake Engineering & Structural Dynamics, Vol. 27, No. 1*.
33. Elmenshawi, A., Sorour, M., Mufti, A., Jaeger, L.G. and Shrive, N. (2010). "Damping Mechanisms and Damping Ratios in Vibrating Unreinforced Stone Masonry", *Engineering Structures, Vol. 32, No. 10*.